Analysis of Three-Dimensional Separated Flow with the Boundary-Layer Equations

David E. Edwards* and James E. Carter†
United Technologies Research Center, East Hartford, Connecticut
and
Frank T. Smith‡
University College London, London, England

An analysis based on the boundary-layer equations is presented for the prediction of three-dimensional separated flow. In this analysis, the boundary-layer equations are solved with finite-difference techniques in four inverse (pressure unknown) modes. One inverse mode, in which the component of vorticity normal to the surface is specified at the boundary-layer edge, is shown to result in an elliptic system of boundary-layer equations and has departure solutions when solved with a forward-marching technique. The accuracy of the present analysis in the other three inverse modes using forward-marching techniques is demonstrated for 1) separated flow over an infinite swept wing that has been rendered three-dimensional with a rotated coordinate system; and 2) a three-dimensional separated flow problem analyzed with an alternate inverse method similar to the triple-deck method of Smith. The principal conclusion of this paper is that several forward-marching techniques are now in place to solve the laminar, incompressible boundary-layer equations for three-dimensional separated flow, and hence future work should focus on the development of three-dimensional viscous-inviscid interaction procedures.

I. Introduction

VISCOUS effects can have a substantial impact on the aerodynamic performance of external and internal flow configurations. For a significant number of high-Reynolds-number flows of practical interest, the viscous effects, even in the presence of boundary-layer separation, are confined to a relatively thin layer near the surface. Many aerodynamic problems can be represented by the interacting boundary-layer theory (IBLT), whereby the flow is divided into regions of viscous and inviscid flows with the two regions coupled through the viscous displacement thickness. It is clear from previous work (see Ref. 1 for a review) that many two-dimensional separated flows can be solved accurately (neglecting the problems of modeling the turbulence and transition processes) through the use of IBLT. However, a majority of the strongly interacting flows of practical interest are three-dimensional, and hence it is timely to turn our attention to the analysis of these flows.

During the past five years, there have been several research efforts directed toward the extension of the IBLT approach to three-dimensional flows. The principal focus of that work has been to develop viscous techniques that can be applied in the analysis of three-dimensional separated flow. Cousteix and Houdeville[2] examined the occurrence of singularities that occur near the separation line when an integral form of the three-dimensional boundary-layer equations is solved for a prescribed pressure (referred to as the direct mode). They concluded that these singularities can be avoided when the equations are solved in an inverse mode for a prescribed displacement thickness distribution. Wigton and Yoshihara[3] developed a three-dimensional IBLT procedure that uses an inverse integral boundary-layer method to represent the viscous region and the full potential equation to represent the inviscid region. They applied their procedure to analyze a wing/fuselage configuration in transonic flow. Delery and Formery[4] developed a three-dimensional inverse finite-difference boundary-layer method that was used to analyze the incompressible flow over an infinite swept wing and the three-dimensional flow in the stagnation region of a wing/plate juncture. The results of Refs. 3 and 4 demonstrated that the three-dimensional boundary-layer equations solved in an inverse mode could be used to avoid the Goldstein singularity at separation. However, the recent work of Wai and Yoshihara[5] and Smith[6,7] has raised questions about the applicability of an inverse boundary-layer analysis for three-dimensional flow. Wai and Yoshihara encountered numerical problems with an IBLT method that used an inverse integral boundary-layer method for the analysis of transonic separated flow. Furthermore, Smith's work has indicated a more fundamental problem that must be addressed in the development of inverse boundary-layer methods for three-dimensional flows. Based on his analysis of the laminar triple-deck equations, Smith has suggested that the inverse form of the three-dimensional boundary-layer equations is of an elliptic nature and hence will result in departure solutions with a forward-marching technique.

It is concluded from the investigations discussed previously that it is not currently clear as to whether or not stable solutions can be obtained for the inverse three-dimensional boundary-layer equations with a forward-marching technique similar to that used extensively in two-dimensional flow. The overall objective of this study is to attempt to clarify this situation by the development and demonstration of several three-dimensional boundary-layer procedures, which can be used subsequently in an IBLT method, for the analysis of strongly interacting flow including boundary-layer separation. Finite-difference techniques have been applied in order to obtain numerically exact solutions of the boundary-layer equations and thereby avoid any singularities or other mathematical behavior that could be introduced by integral formulations of the boundary-layer equations. This initial research thrust in three-dimensional separated flow is limited to closed, laminar separation bubbles that occur on solid

Presented as Paper 85-1499 at the AIAA Seventh Computational Fluid Dynamics Conference, Cincinnati, OH, July 15-17, 1985; received Aug. 5, 1985; revision submitted March 14, 1986.

*Research Engineer. Member AIAA.
†Manager, Computational Fluid Dynamics. Member AIAA.
‡Professor, Department of Mathematics.

surfaces, thereby avoiding the issues that arise in open separation problems (discussed by Wang[8]) and the complex topology (see Ref. 9) that occurs for general three-dimensional separated flows.

In this study, the boundary-layer equations are solved in four different inverse modes, designated as Inverse I–IV; two integral thicknesses are prescribed in Inverse I, an integral thickness and one component of edge velocity are prescribed in Inverse II, the displacement thickness as defined by Moore[10] and one component of edge velocity are prescribed in Inverse III, and the displacement thickness and the edge component of vorticity normal to the surface are prescribed in Inverse IV. Each inverse mode results in a different system of three-dimensional boundary-layer equations. The Inverse IV mode is shown to lead to an elliptic system of equations, and hence the use of a forward-marching technique leads to departure solutions that are supported by numerical computation. In contrast, Inverse modes I–III are shown to yield stable solutions with forward-marching techniques. The accuracy of the boundary-layer equations solved in Inverse I–III modes is demonstrated for a closed-separation bubble on an infinite swept wing. Comparisons are presented between infinite swept wing results and three-dimensional solutions obtained from the present formulation in a coordinate system that has been rotated to render the problem three-dimensional. In addition, for a fully three-dimensional laminar separated flow at finite Reynolds number, comparisons are presented with an alternate inverse boundary-layer procedure, which is described in the Appendix. Two principal conclusions have been made in this study. First, the inverse boundary-layer equations solved subject to the specification of the edge component of vorticity normal to the surface results in an elliptic system of equations; these must be avoided if a forward-marching technique is to be applied. Second, the viscous methodology presented herein is now in place for the future development of an IBLT analysis for three-dimensional incompressible, laminar, separated flows.

II. Analysis

In this section, the formulation of the viscous flow equations, simplified for incompressible, laminar flow, is presented. Different systems of the boundary-layer equations are formed in which each system depends upon the conditions specified at the boundary-layer edge. In addition, a brief examination is made as to the underlying mathematical character of these formulations.

Viscous Formulation

The flow in the viscous region is assumed to be governed by Prandtl's boundary-layer equations expressed in x, y, and z coordinates, where x is the distance along the surface, y is the distance normal to the surface, and z is the surface distance in the spanwise direction; u, v, and w are the velocity components in the x, y, and z directions, respectively, as shown in Fig. 1. The nondimensional incompressible boundary-layer equations in the present study are represented by two stream-function definitions and two momentum equations, written as

$$\frac{\partial \psi}{\partial \eta} = hu \tag{1}$$

$$\frac{\partial \phi}{\partial \eta} = hw \tag{2}$$

$$h^2 u\frac{\partial u}{\partial x} - h\left(\frac{\partial \psi}{\partial x} + \frac{\partial \phi}{\partial z}\right)\frac{\partial u}{\partial \eta} + h^2 w\frac{\partial u}{\partial z} = h^2\left(u_e\frac{\partial u_e}{\partial x} + w_e\frac{\partial u_e}{\partial z}\right) + \frac{\partial^2 u}{\partial \eta^2} \tag{3}$$

$$h^2 u\frac{\partial w}{\partial x} - h\left(\frac{\partial \psi}{\partial x} + \frac{\partial \phi}{\partial z}\right)\frac{\partial w}{\partial \eta} + h^2 w\frac{\partial w}{\partial z} = h^2\left(u_e\frac{\partial w_e}{\partial x} + w_e\frac{\partial w_e}{\partial z}\right) + \frac{\partial^2 w}{\partial \eta^2} \tag{4}$$

and y, v, ψ, and ϕ have been scaled in the usual manner by $\sqrt{Re}$, where Re is the Reynolds number. The continuity equation is automatically satisfied through the use of the functions ψ and ϕ, which are related to the normal velocity component v shown in Fig. 1 by

$$v = -\left(\frac{\partial \psi}{\partial x} + \frac{\partial \phi}{\partial z}\right) \tag{5}$$

The normal coordinate $\eta = y/h$, where $h = h(x, z)$, is introduced to reduce the boundary-layer growth in the η coordinate. Boundary conditions for the foregoing viscous equations are given by

$$\eta = 0, \qquad u = w = \psi = \phi = 0 \tag{6}$$

at the surface, and by

$$\eta \to \infty, \qquad u \to u_e \qquad w \to w_e \qquad \psi \to u_e y - u_e\delta_1 \qquad \phi \to w_e y - u_e\delta_2 \tag{7}$$

at the boundary-layer edge, where the integral thicknesses δ_1 and δ_2 are defined as

$$\delta_1 = \int_0^\infty \left(1 - \frac{u}{u_e}\right) dy \qquad \delta_2 = \int_0^\infty \left(\frac{w_e - w}{u_e}\right) dy \tag{8}$$

For three-dimensional flows, Moore[10] deduced that the displacement thickness δ^* is governed by a partial-differential equation which, for incompressible flow, is written as

$$\frac{\partial}{\partial x}[u_e(\delta^* - \delta_x)] + \frac{\partial}{\partial z}[w_e(\delta^* - \delta_z)] = 0 \tag{9}$$

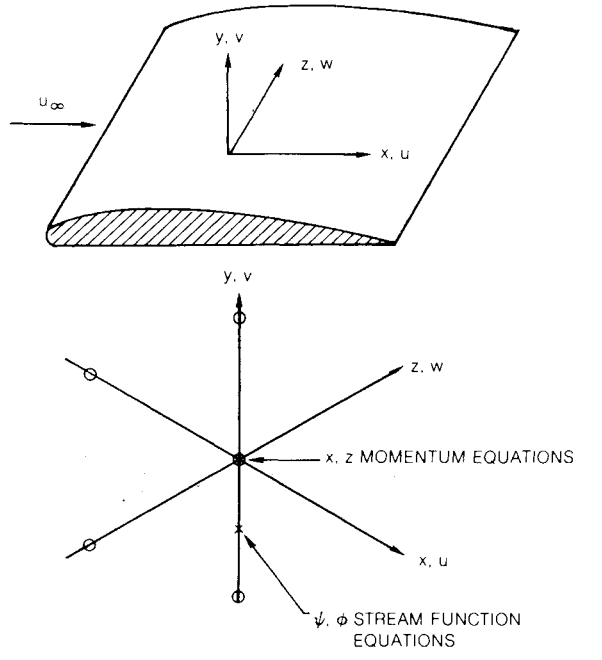

Fig. 1 Coordinate system for three-dimensional boundary-layer equations and finite-difference computational molecule ($w > 0$).

where Moore defined the integral thicknesses δ_x and δ_z as

$$\delta_x = \int_0^\infty \left(1 - \frac{u}{u_e}\right) dy \qquad \delta_z = \int_0^\infty \left(1 - \frac{w}{w_e}\right) dy \quad (10)$$

Moore's integral thicknesses are related to those in the present study by $\delta_x = \delta_1$ and $\delta_z = (u_e/w_e)\delta_2$, and hence Eq. (9) can be rewritten as

$$\frac{\partial}{\partial x}[u_e(\delta^* - \delta_1)] + \frac{\partial}{\partial z}(w_e\delta^* - u_e\delta_2) = 0 \quad (11)$$

A system of equations with u, w, ψ, ϕ, δ_1, δ_2, and δ^* as unknowns is formed from Eqs. (1–4) and (11) subject to the boundary conditions given in Eqs. (6) and (7). Two additional conditions must be specified to close the system of equations. The boundary-layer equations in this study are solved in the direct mode and four inverse modes with the conditions shown in Table 1, where each mode represents a different closed system of boundary-layer equations. Either an integral quantity or a component of edge velocity is specified in the Inverse I–III modes to close the system of equations. For the Inverse IV mode, the displacement thickness δ^* and the component of edge vorticity normal to the surface Ω_y is specified. Setting $\Omega_y = 0$ in the Inverse IV mode forces the flow to be irrotational at the boundary-layer edge.

The boundary-layer equations have been discretized with a finite-difference approach, in which derivatives in the x and z directions have first-order approximations, and derivatives in the η direction have second-order approximations. Figure 1 also shows the computational molecule used in the present technique. It is seen in this figure that the two stream functions are evaluated at half a grid spacing below where the momentum equations are evaluated. The computational molecule is shown with a backward difference for z derivatives which assumes that $w > 0$; if $w \leq 0$, then a forward-difference approximation is used for the z derivatives, as suggested by Krause.[11] If $u \leq 0$, then the x-convection terms in both momentum equations are set to zero in order to avoid stability problems in a fashion similar to the FLARE approximation[12] used in two-dimensional flows. In the future, this approximation will be replaced with upwind differencing. Newton linearization is applied to the finite-difference equations at each surface station as the solution is marched from either two planes of initial data or a plane of initial data and a plane of symmetry.

The resulting set of linearized equations is block (4×4) tridiagonal and is solved with a block form of the Thomas algorithm. The recurrence constants used in the back substitution procedure are computed from the surface to the boundary-layer edge. At the edge of the boundary layer, two additional conditions are specified in order to determine the solution of the viscous system. For example, in the direct mode u_e and w_e are specified to close the system of equations. Similarly, in the Inverse IV mode δ^* and Ω_y are specified. In each mode the specification of two conditions permits the surface-dependent variables (u_e, w_e, δ_1, δ_2, and δ^*) to be deduced. The boundary-layer solution is then completed by the usual back substitution process from the viscous edge to the surface to obtain u, w, ψ, and ϕ.

Table 1 Direct and inverse solution modes for the three-dimensional boundary-layer equations

Mode	Conditions specified
Direct	u_e, w_e
Inverse I	δ_1, δ_2
Inverse II	δ_1, w_e
Inverse III	δ^*, w_e
Inverse IV	$\delta^*, \Omega_y = \frac{\partial u_e}{\partial z} - \frac{\partial w_e}{\partial x}$

An Elliptic System of Three-Dimensional Boundary-Layer Equations

Recently, the work of Smith[6,7] and Sykes[13] on the triple-deck equations has strongly suggested that the system of three-dimensional boundary-layer equations is elliptic if solved in an inverse mode. In this case, conventional forward-marching techniques cannot be applied, since departure solutions will result. Departure solutions are those that result when small changes in the initial conditions lead to massive changes in the solution downstream because of the treatment of a boundary-value problem with an initial value solution technique. However, there are several efforts recently reported in the literature in which stable, finite-difference solutions to the three-dimensional inverse boundary-layer equations using a forward-marching technique were obtained. For example, Delery and Formery[4] did not encounter departure solutions to the three-dimensional boundary-layer equations in their use of a formulation similar to Inverse I in the present paper and also of an inverse formulation in which the components of wall shear were prescribed. Steger and Van Dalsem[14] avoided possible forward-marching instabilities because they employed a time-relaxation algorithm to obtain inverse solutions to the three-dimensional boundary-layer equations. A question that therefore arises is whether the ellipticity in the system of three-dimensional inverse boundary-layer equations is a general property or is dependent upon the particular inverse formulation that is applied. Similar issues arise in the treatment of the integral form of the three-dimensional boundary-layer equations. For example, Wigton and Yoshihara[3] indicated that the integral formulations of the inverse boundary-layer equations of Cousteix and Houdeville[2] (in which two integral thicknesses are specified) and of Smith[15] (in which the displacement thickness and edge component of vorticity normal to the surface are prescribed) result in a nonhyperbolic system of equations for three-dimensional flows. Wigton and Yoshihara[3] were able, after much experimentation, to deduce an integral formulation, in which a shape factor and flow angle were specified, which resulted in a hyperbolic system that permits the use of a forward-marching technique.

One of the objectives of the present study is to perform numerical studies using a forward marching technique to determine which, if any, of the present inverse formulations will have departure solutions. Whether or not a marching procedure is stable could also be found by determining the characteristic slopes for the given set of equations. If all of the slopes are real (indicating a fully hyperbolic system), then a marching procedure is permitted, provided that the initial data lines are properly space-like. If, however, some of the slopes are complex, the system of equations is partially elliptic, and thus a forward-marching technique cannot be applied. Integral formulations of the three-dimensional boundary-layer equations lend themselves rather easily to a characteristic analysis; finite-difference formulations are more complicated, and hence in this investigation numerical studies for departure solutions are used. In addition to these numerical studies, the results of which are presented in the next section, an analytical observation was made which clarifies the issue of whether or not departure solutions will occur for the inverse three-dimensional boundary-layer equations. This observation is made relative to the Inverse IV mode used in the present study. In this mode, the edge value of the component of vorticity normal to the surface, which is written as

$$\frac{\partial u_e}{\partial z} - \frac{\partial w_e}{\partial x} = \Omega_y \quad (12)$$

is a specified condition for the solution of the three-dimensional boundary-layer equations. Furthermore, at the

boundary-layer edge, the continuity equation becomes

$$\frac{\partial u_e}{\partial x} + \frac{\partial v_e}{\partial y} + \frac{\partial w_e}{\partial z} = 0 \tag{13}$$

If Ω_y is denoted as $f(x,z)$ and $-(\partial v_e/\partial y)$ as $g(x,z)$, then Eqs. (12) and (13) can be written as

$$\frac{\partial u_e}{\partial z} - \frac{\partial w_e}{\partial x} = f(x,z) \tag{14}$$

$$\frac{\partial u_e}{\partial x} + \frac{\partial w_e}{\partial z} = g(x,z) \tag{15}$$

which is a set of two linear equations for the two unknowns u_e and w_e. It is immediately observed that the homogeneous equations to Eqs. (14) and (15) are the Cauchy-Riemann equations, thereby indicating that the homogeneous solutions for u_e and w_e are governed by Laplace's equation, and hence Eqs. (14) and (15) are elliptic. Although the actual numerical procedure used to deduce u_e and w_e was that described in the previous section, this analytical observation strongly suggests that the Inverse IV formulation results in a boundary-value rather than an initial-value problem. Numerical studies described in the next section offer further verification that the Inverse IV formulation leads to an elliptic system and that the use of a forward-marching technique results in departure solutions.

An alternate inverse method, which is a generalization of a triple-deck method developed by Smith to solve the three-dimensional finite-Reynolds-number boundary-layer equations, is presented in the Appendix. Results obtained with this procedure are used for comparison in Sec. III with those results obtained with the Inverse I–III methods. This alternate approach renders the problem elliptic, since the pressure is deduced from a Poisson equation that is obtained by differentiating the x- and z-momentum equations with respect to x and z, respectively. In contrast, the pressure does not explicitly appear in the Inverse I–IV formulations, since it has been replaced with the gradients of the boundary-layer edge velocity components. In the Inverse I–IV procedures, the pressure can be deduced from Bernoulli's equation after u_e and w_e are computed, provided that the flow at the viscous edge is irrotational. It is noted that only in the Inverse IV procedure can the flow at the viscous edge be specified to be irrotational, thereby permitting the direct computation of pressure. However, the Inverse IV formulation, as shown in the next section, does not result in a well-posed initial-value problem. This suggests that the treatment of the pressure in an inverse formulation will determine whether or not a forward-marching technique can be applied in solving the system of three-dimensional boundary-layer equations. Specifically, if the pressure explicitly appears as an unknown or can be obtained directly from the solution, the problem is rendered a boundary-value problem. Alternatively, if only the edge velocity components, but not the pressure, are computed, then a well-posed initial-value problem is obtained.

III. Results and Discussion

In this section, results are presented which demonstrate that departure solutions are obtained in the solution of the boundary-layer equations in the Inverse IV mode. A simple three-dimensional laminar accelerating flow is used to demonstrate this fact. In addition, the accuracy of the other three methods (Inverse I–III) is demonstrated through the analysis of several laminar incompressible separated flows with known numerical solutions. The first flow case is the separated flow over an infinite swept wing which has been recast into a new coordinate system to make the problem three-dimensional. Comparisons are made with solutions obtained from an infinite swept wing (ISW) analysis that has been recast into the rotated system. The second flow case is a fully three-dimensional separated flow generated by using the alternate inverse method described in the Appendix. All calculations were made in double precision on a 32-bit APOLLO DN 460 computer.

Departure Solutions to the Three-Dimensional Boundary-Layer Equations

The flow that is used in this numerical study of departure solutions is an accelerating flow over a flat plate. The computational range is $1.0 < x < 1.75$, $0 < z < 0.55$, and $0 < \eta < 10$, with $h = 1$. The flow is assumed to be a Blasius flat-plate boundary layer up to $x = 1$, with symmetry conditions at $z = 0$. Calculations were made using a uniform grid in each direction, where 151, 12, and 21 points were used in the x, z, and y directions, respectively. In this computational region, w_e is defined as

$$w_e = \tfrac{2}{3}(x-1)^3 z \tag{16}$$

The edge velocity component u_e was deduced from the numerical integration of Eq. (12), in which Ω_y had been set to zero. With $u_e = 1$ at $x = 1$, and $u_e = 1$ at $z = 0$, u_e is obtained from

$$\frac{\partial u_e}{\partial z} = \frac{\partial w_e}{\partial x} \tag{17}$$

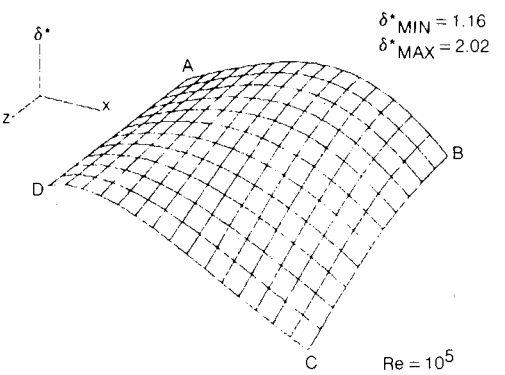

a) Displacement thickness.

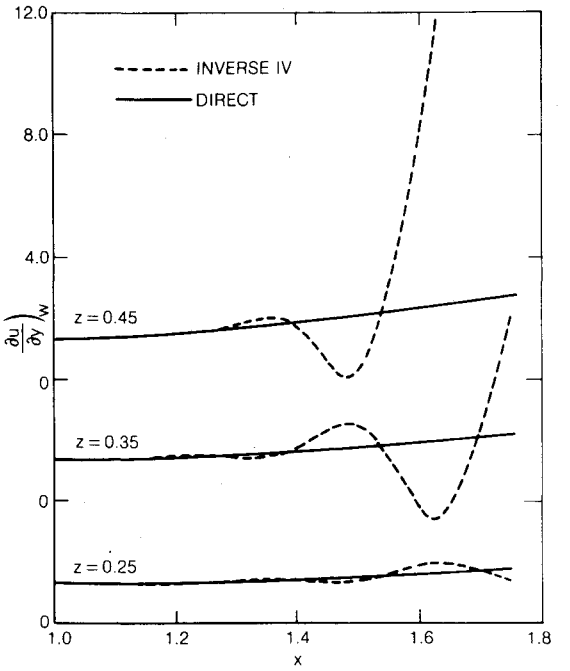

b) x component of wall shear.

Fig. 2 Accelerating flow test case used to study departure solutions.

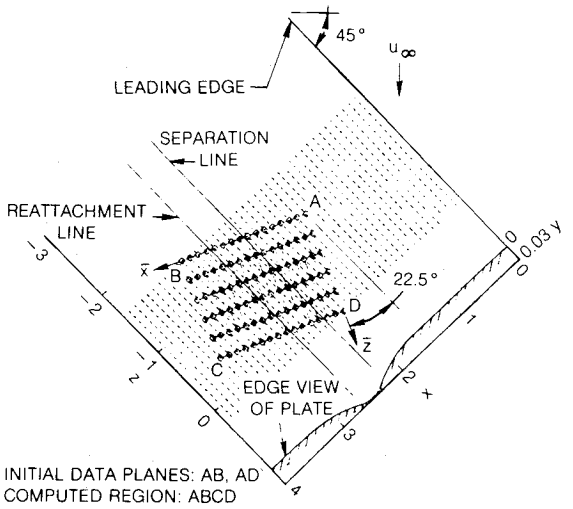

Fig. 3 Schematic diagram of swept plate with trough.

using one-sided differencing. The boundary-layer equations were solved in the direct mode to provide quantities to be used in the various inverse modes. The displacement thickness δ^* is obtained from the solution, since Moore's[10] differential equation for δ^* is part of the system of boundary-layer equations, and is shown in Fig. 2a, where AD is the initial data line at $x = 1$, and AB is the symmetry line at $z = 0$. Figure 2a shows that the overall trend is for the displacement thickness to decrease in the mainstream direction, as expected for an accelerating flow.

The boundary-layer equations were then solved in all four inverse modes, using the required prescribed quantities obtained from the direct calculation. The results of all inverse calculations were identical to the direct results. The integral quantities δ_1, δ_2, and δ^* were then perturbed by 1% at $x = 1.005$ and $z = 0.1$, and the boundary-layer equations were again solved in all inverse modes. The results of the Inverse I–III calculations were essentially identical to the direct results. However, the Inverse IV results exhibited a catastrophic departure from the direct solution, as seen in Fig. 2b for the distribution of the x component of wall shear along lines of constant z. From Fig. 2b it is observed that the error along each z line is growing as a sinusoidal wave, with the amplitude of the wave growing exponentially.

Additional calculations were made for the three-dimensional boundary-layer equations using Inverse I–III modes in which δ_1, δ_2, and δ^* were perturbed by as much as 10% at $x = 1.005$ and $z = 0.1$. No departure solutions were observed in the calculations. It is concluded from this numerical study, as well as others that have been performed, that the Inverse modes I–III form properly posed initial-value problems that can be solved in a stable manner with forward-marching techniques. In contrast, the specification of the edge component of vorticity normal to the surface renders the system of three-dimensional boundary-layer equations elliptic, thereby leading to departure solutions with the use of forward-marching techniques. For the remaining flow problems to be studied, the Inverse IV mode will not be used.

Separated Flow over a Swept Plate with Trough

The first separated flow case to be presented is that of a laminar separated flow over an infinite flat plate with a trough located downstream of the plate leading edge which is swept 45 deg with respect to the freestream direction. The trough has a nondimensional depth of 0.03. A schematic diagram of the configuration is shown in Fig. 3. A known solution, for comparison purposes, is obtained from an infinite swept wing (ISW) analysis of this swept separated flowfield. This ISW

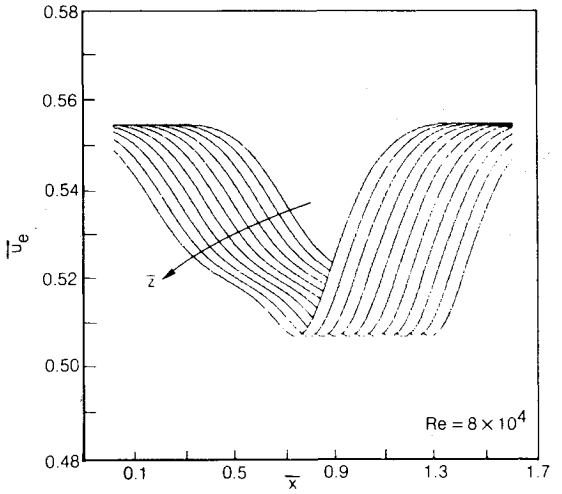

a) Edge velocity in $\bar{x}$ direction.

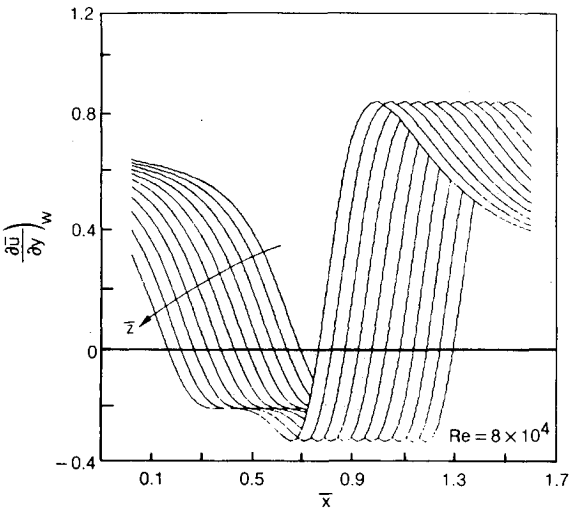

b) $\bar{x}$ component of wall shear.

Fig. 4 Infinite swept-wing results rotated 22.5 deg for flow over 45-deg swept plate with trough.

analysis is obtained by setting the z derivatives to zero in the Inverse III method. The inverse boundary-layer solution is obtained by prescribing the displacement thickness deduced in Ref. 16 for the two-dimensional flow over this trough configuration. For the conditions of an infinite swept wing, Eq. (11) shows that the three-dimensional δ^* reduces to the usual two-dimensional definition given by δ_1 in Eq. (8). Several three-dimensional analyses using the present methods are made in the $(\bar{x}, \bar{z}, \eta)$ coordinate system, which has been rotated 22.5 deg from the original coordinate system (x, z, η) in order to make the problem fully three-dimensional. The computational region for the present analysis is designated as $ABCD$ in Fig. 3. The ISW solution has been used to provide the initial data planes at AB and AD, as well as the required integral quantities and edge velocity components at each grid point in the calculation. Interpolation has been avoided by setting a constant step size of 0.0271 in the $\bar{x}$ direction and 0.0653 in the $\bar{z}$ direction, which corresponds to the step size of 0.025 in the x direction used in the ISW analysis. For both the ISW and three-dimensional calculations, the same normal grid was used. The three-dimensional calculation used 61, 21, and 56 points in the $\bar{x}$, $\bar{z}$, and η directions, respectively.

The results of the ISW calculation rotated 22.5 deg into the $(\bar{x}, \bar{z}, \eta)$ system and the three-dimensional boundary-layer equations solved in the Inverse III mode are shown in Figs. 4 and 5, respectively. The solutions for the Inverse modes I–III

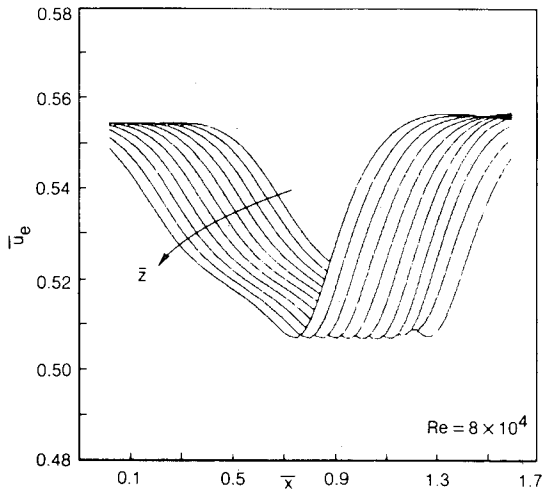

a) Edge velocity in $\bar{x}$ direction.

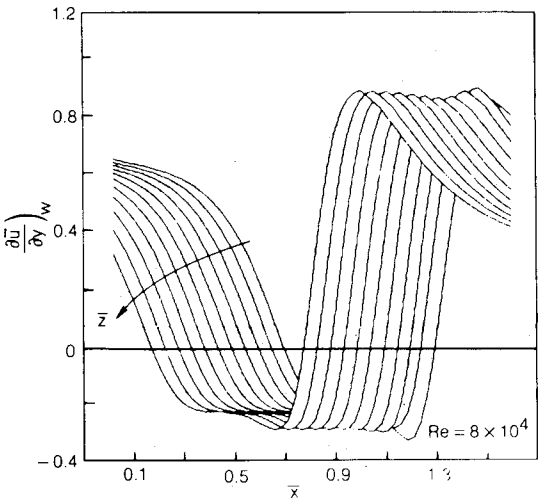

b) $\bar{x}$ component of wall shear.

Fig. 5 Inverse III results for flow over 45-deg swept plate with trough.

are nearly the same; hence only the Inverse III results are shown. Figures 4a and 5a show the distribution of $\bar{u}_e$, the edge component of velocity in the $\bar{x}$ direction, along lines of constant $\bar{z}$. Figures 4b and 5b show the distribution of $(\partial \bar{u}/\partial y)_w$ at the wall along lines of constant $\bar{z}$. Comparison of results in these figures shows that good agreement is obtained between the three-dimensional results and the rotated ISW results. The results are essentially identical in the attached flow region; in the separated flow region there is a slight difference, since the implementation of the FLARE approximation in the ISW equations differs somewhat from the FLARE approximation in the three-dimensional equations. This minor problem will be eliminated in the future through the use of proper windward differencing in the three-dimensional analysis.

Three-Dimensional Separated Flow Model Problem

A three-dimensional laminar separated flow problem was generated using the alternate inverse boundary-layer method described in the Appendix. In this alternate method, a quasi-displacement function G is prescribed for this problem and is given by the relation

$$G(x,z) = 2\exp\left\{-\left[(x-1.5)^2 + z^2\right]/0.04\right\} \qquad (18)$$

The calculated flowfield solution from the alternate method has been used to provide the required input quantities for use

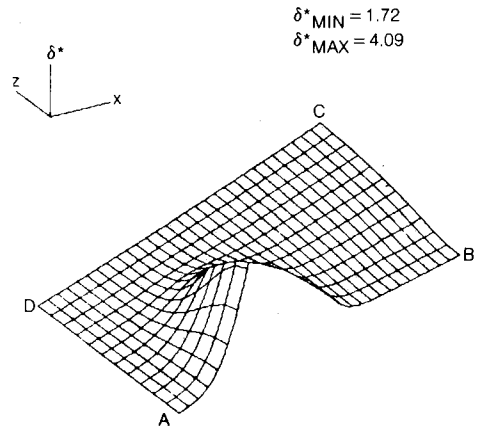

a) Prescribed displacement thickness.

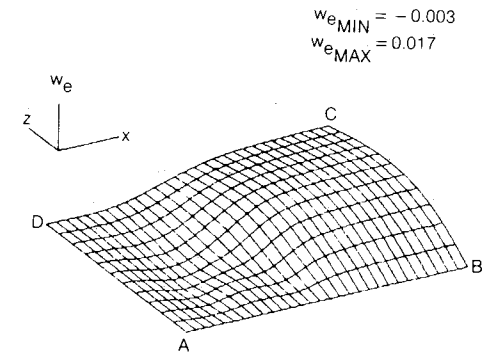

b) Edge velocity in z direction.

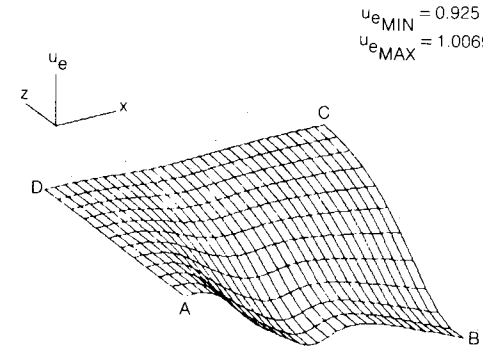

c) Edge velocity in x direction.

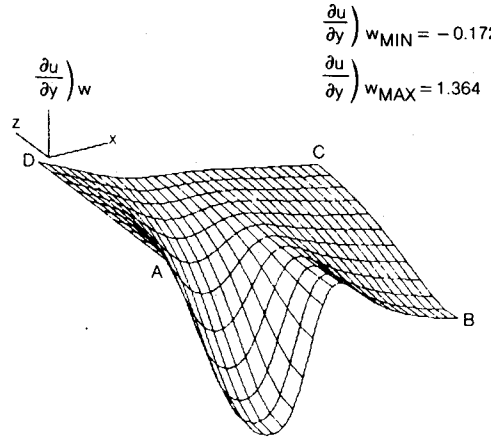

d) x component of wall shear.

Fig. 6 Three-dimensional separated flow case ($Re = 10^5$).

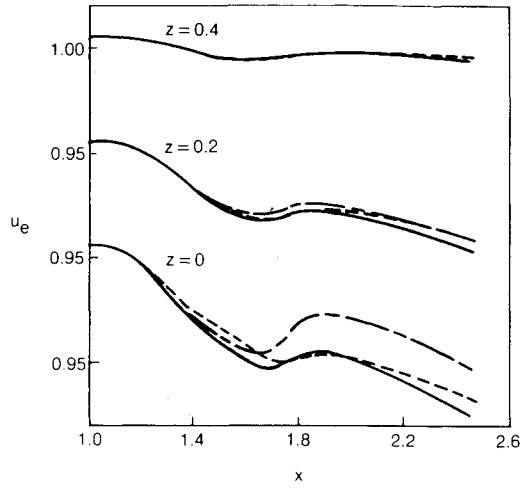

a) Edge velocity in x direction.

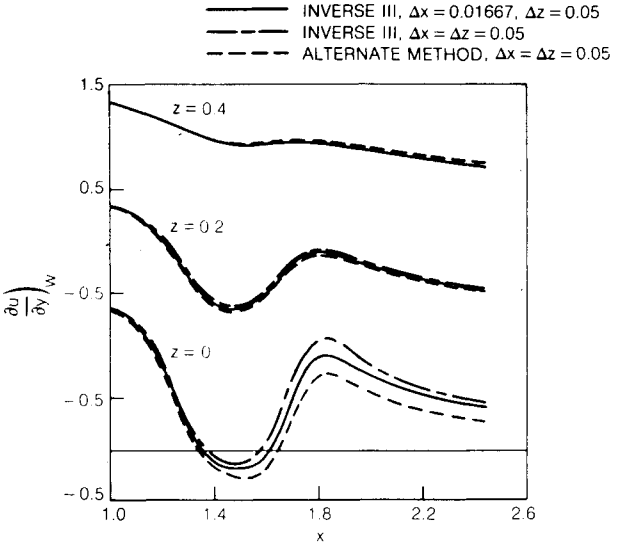

b) x component of wall shear.

Fig. 7 Comparison of inverse boundary-layer results ($Re = 10^5$).

in the Inverse I–III methods. The computational range is $1 < x < 2.45$, $0 < z < 0.55$, and $0 < \eta < 10$, with $h = 1$. The flow is assumed to be a Blasius flat-plate boundary layer up to $x = 1$, with a plane of symmetry at $z = 0$. The displacement thickness δ^* and edge component of velocity w_e, which were deduced from the alternate solution, are shown in Figs. 6a and 6b, respectively. In these figures, AD is the initial data line at $x = 1$ and AB is the symmetry line at $z = 0$. The three-dimensionality of this flow is further demonstrated in Figs. 6c and 6d, where the distributions of the component of edge velocity u_e and x component of wall shear $(\partial u/\partial y)_w$ from this flow are shown. From these two figures, it is observed that along the plane of symmetry AB there is an adverse pressure gradient $(\partial u_e/\partial x < 0)$, resulting in a separated flow region $[(\partial u/\partial y)_w < 0]$. The size of the adverse pressure gradient decreases as z increases, which results in a separated flow region near $z = 0$, with attached flow away from the plane of symmetry.

A calculation using the present method was made on this flow in each of the inverse modes. This calculation used uniform grids in each direction, with 30, 12, and 21 grid points in the x, z, and η directions, respectively, resulting in the same step size as the alternate method. Since the present method is first-order accurate in the x and z directions and the alternate method is second-order accurate in all directions, a second calculation, with the x grid refined, was made to determine the effect that the step size in the x direction has on the accuracy of the solution. The second calculation used uniform grids in each direction, with 88, 12, and 21 grid points in the x, z, and η directions, respectively. Again, the solutions for the Inverse modes I-III are nearly the same, and thus only the Inverse III results are shown.

Comparison of the results of the Inverse III analysis using both a coarse and fine x grid with the results of the alternate method is shown in Fig. 7, where distributions of the component of edge velocity u_e and the x component of wall shear $(\partial u/\partial y)_w$ for $z = 0$, 0.2, and 0.4 are shown in Figs. 7a and 7b, respectively. The results of the present analysis using the coarse mesh are in fair agreement with the results of the alternate method, with the largest discrepancy occurring in the separated region near the plane of symmetry. The agreement shown in Figs. 7a and 7b between the present results and the alternate method results is substantially improved with the use of a finer step size in the x direction in the present first-order method. The present computation was repeated with a finer step size in the z direction; only minor changes were observed in the results. Overall, the present comparison with the alternate method is considered quite encouraging, as these two three-dimensional boundary-layer procedures differ substantially. If it were desired, a more precise comparison of the accuracy of the present method and the alternate method would require a detailed grid refinement study of both methods.

IV. Concluding Remarks

An analysis based on the boundary-layer equations has been presented for the prediction of three-dimensional separated flow. In this study, finite-difference techniques were used to solve the boundary-layer equations in four different inverse modes, designated as Inverse I–IV; two integral thicknesses are prescribed in Inverse I, an integral thickness and one component of edge velocity are prescribed in Inverse II, the displacement thickness and one component of edge velocity are prescribed in Inverse III, and the displacement thickness and the edge component of vorticity normal to the surface are prescribed in Inverse IV. Each inverse mode results in a different system of three-dimensional boundary-layer equations. The Inverse IV mode was shown to lead to an elliptic system of equations, and hence the use of a forward-marching technique was found to result in departure solutions. The other three methods (Inverse I–III), which were solved using a forward-marching technique, were shown to produce stable, accurate results for several laminar incompressible separated flows with known numerical solutions. The first flow case was the separated flow over an infinite swept wing recast into a new coordinate system to make the problem three-dimensional. The second flow case is a truly three-dimensional separated flow.

Two principal conclusions have been made in this study. First, the inverse boundary-layer equations solved subject to the specification of the edge component of vorticity normal to the surface result in an elliptic system of equations and must be avoided if a forward-marching technique is to be used. Second, the viscous methodology is now in place for the future development of an IBLT analysis for three-dimensional laminar, incompressible separated flows.

Appendix: Alternate Inverse Method

The alternate inverse method outlined here is based on the triple-deck method described in Ref. 7. It is designed to honor the ellipticity and avoid the branching when the total displacement thickness is prescribed and the pressure is to be found.

The governing equations and boundary conditions are considered in the form

$$\frac{\partial u}{\partial x}+\frac{\partial v}{\partial y}+\frac{\partial w}{\partial z}=0 \tag{A1}$$

$$u\frac{\partial u}{\partial x}+v\frac{\partial u}{\partial y}+w\frac{\partial u}{\partial z}=\frac{-\partial p}{\partial x}+\frac{\partial^2 u}{\partial y^2} \tag{A2}$$

$$u\frac{\partial w}{\partial x}+v\frac{\partial w}{\partial y}+w\frac{\partial w}{\partial z}=-\frac{\partial p}{\partial z}+\frac{\partial^2 w}{\partial y^2} \tag{A3}$$

$$u=v=w=0 \quad \text{at} \quad y=0 \tag{A4}$$

$$u\to u_e, \quad w\to w_e,$$

$$v\sim -y\left(\frac{\partial u_e}{\partial x}+\frac{\partial w_e}{\partial z}\right)+\frac{\partial G u_e}{\partial x}+\frac{\partial G w_e}{\partial z} \quad \text{as} \quad y\to\infty \tag{A5}$$

with the quasi-displacement function $G(x,z)$ prescribed, whereas the pressure p and edge velocities u_e and w_e are unknown. In the current method, the skewed shears

$$\bar{u}=\frac{\partial u}{\partial x}+\frac{\partial w}{\partial z}, \qquad \bar{v}=\frac{\partial v}{\partial x} \tag{A6}$$

are introduced. Then, the x,z derivatives of Eqs. (A2) and (A3) in turn give, on addition,

$$\frac{\partial \bar{u}}{\partial x}+\frac{\partial \bar{v}}{\partial y}=0 \tag{A7}$$

$$u\frac{\partial \bar{u}}{\partial x}+\bar{v}\frac{\partial u}{\partial y}=-\bar{e}+\frac{\partial^2 \bar{u}}{\partial y^2}-\sigma \tag{A8}$$

subject to

$$\bar{u}=\bar{v}=0 \quad \text{at} \quad y=0 \tag{A9}$$

$$\bar{u}\to\bar{u}_e, \qquad \bar{v}+(y-G)\frac{\partial \bar{u}_e}{\partial x}\to H \quad \text{as} \quad y\to\infty \tag{A10}$$

with $\bar{u}_e(x,z)$ unknown. Here σ consists of a host of nonlinear terms:

$$\sigma=\left(\frac{\partial u}{\partial x}\right)^2+v\frac{\partial^2 u}{\partial x\partial y}+2\frac{\partial w}{\partial x}\frac{\partial u}{\partial z}+w\frac{\partial^2 u}{\partial x\partial z}+\frac{\partial}{\partial z}\left(v\frac{\partial w}{\partial y}\right)+\frac{\partial}{\partial z}\left(w\frac{\partial w}{\partial z}\right) \tag{A11}$$

which triple-deck theory indicates are in some sense secondary to the inverse calculation, at least for small disturbances. Also, H and $\bar{e}$ are defined by

$$H=u_e\frac{\partial^2 G}{\partial x^2}+2\frac{\partial u_e}{\partial x}\frac{\partial G}{\partial x}+\frac{\partial}{\partial z}\left(w_e\frac{\partial G}{\partial x}\right)+\frac{\partial G}{\partial z}\frac{\partial w_e}{\partial x} \tag{A12}$$

$$\nabla^2 p=\bar{e} \tag{A13}$$

The simple Poisson relation, Eq. (A13), between $\bar{e}$ and p in fact captures all of the ellipticity of this inverse procedure.

The method then proceeds as follows:

1) Using Eqs. (A7–A10), set a computational problem for $\bar{u}$, $\bar{v}$, and $\bar{e}$, with other quantities (i.e., u, v, w, σ, and H) assumed known at their latest or starting values. Equations (A7–A10) are solved by quasi-two-dimensional sweeps of the boundary layer, forward in x, at each z.

2) Equation (A13) is used to update the pressure field p from the latest $\bar{e}$ distribution using Gauss-Siedel sweeps in x and z.

3) Equation (A3) is solved subject to the constraints on w in Eqs. (A4) and (A5) to provide new values of w and w_e, with all else assumed known.

4) Integration of Eq. (A6) then yields updated u, u_e, and v distributions.

5) σ and H are recalculated from Eqs. (A11) and (A12).

6) Go back to step 1, and repeat until convergence.

The finite-differencing taken, which is nominally second-order-accurate in all directions, and the symmetry imposed at $z=0$ are as in Ref. 7. The results from the method are described in the main text of this paper.

Acknowledgments

The work reported in this paper was supported by the Office of Naval Research, with Dr. R. E. Whitehead as Technical Monitor under Contract N00014-81-C-0381. The authors acknowledge the interest and helpful suggestions provided by Drs. M. J. Werle and M. Barnett of United Technologies Research Center.

References

[1] McDonald, H. and Briley, W.R., "A Survey of Recent Work on Interacted Boundary Layer Theory for Flow with Separation," Second Symposium on Numerical and Physical Aspects of Aerodynamic Flows, Long Beach, CA, Jan. 1983.

[2] Cousteix, J. and Houdeville, R., "Singularities in Three-Dimensional Turbulent Boundary Layer Calculations and Separated Phenomena," ONERA Cert. Rep; also AGARD CP 291, 1980.

[3] Wigton, L. and Yoshihara, H., "Viscous-Inviscid Interactions with a Three-Dimensional Inverse Boundary Layer Code," Boeing Co., Rept. D6-51714, 1982; also Second Symposium on Numerical and Physical Aspects of Aerodynamic Flows, Long Beach, CA, Jan. 1983.

[4] Delery, J.M. and Formery, M.J., "A Finite Difference Method for Inverse Solutions of 3-D Turbulent Boundary Layer Flow," AIAA Paper 83-0301, 1983.

[5] Wai, J. and Yoshihara, H., "Transonic Turbulent Separation on Swept Wings—A Return to the Direct Formulation," AIAA Paper 83-0265, 1984.

[6] Smith, F.T., "Theoretical Aspects of Steady and Unsteady Laminar Separation," AIAA Paper 84-1582, 1984.

[7] Smith, F.T., "Properties, and a Finite-Difference Approach, for Interactive Three-Dimensional Boundary Layers," United Technologies Research Center, Rept. 83-46, 1983.

[8] Wang, K.C., "On the Disputes About Open Separation," AIAA Paper 83-0296, 1983.

[9] Tobak, M. and Peake, D.J., "Topology of Two Dimensional and Three Dimensional Separated Flows," AIAA Paper 79-1480, 1979.

[10] Moore, F.K., "Displacement Effect on a Three Dimensional Boundary Layer," NACA Rept. 1124, 1953.

[11] Krause, E., "Comment on Solution of Three-Dimensional Boundary Layer Flow with Separation," *AIAA Journal*, Vol. 7, March 1969, pp. 575–576.

[12] Reyhner, T.A. and Flügge-Lotz, I., "The Interaction of a Shock Wave with a Laminar Boundary Layer," *International Journal of Non-Linear Mechanics*, Vol. 8, No. 2, June 1968, pp. 173–179.

[13] Sykes, R.J., "On Three-Dimensional Boundary Layer Flow Over Surface Irregularities," *Proceedings of the Royal Society (London)*, A373, 1980, pp. 311–329.

[14] Steger, J.L. and Van Dalsem, W.R., "Developments in the Simulation of Separated Flows using Finite Difference Methods," Third Symposium on Numerical Methods and Physical Aspects of Aerodynamic Flows, Long Beach, CA, 1985.

[15] Smith, P.D., "The Numerical Computation of Three Dimensional Turbulent Boundary Layers," Royal Aircraft Establishment, Tech. Memo. Aero 1945, 1982.

[16] Carter, J.E. and Wornon, S.F., "Solution for Incompressible Separated Boundary Layers Including Viscous-Inviscid Interaction," NASA SP-347, 1975.